HHS Public Access

Author manuscript

J Stroke Cerebrovasc Dis. Author manuscript; available in PMC 2018 April 01.

Published in final edited form as:

J Stroke Cerebrovasc Dis. 2017 April ; 26(4): 863–870. doi:10.1016/j.jstrokecerebrovasdis.2016.10.035.

Cryptogenic Stroke and Nonstenosing Intracranial Calcified Atherosclerosis

Hooman Kamel, MD[1,2], **Gino Gialdini, MD**[1], **Hediyeh Baradaran, MD**[3], **Ashley E. Giambrone, PhD**[3,4], **Babak B. Navi, MD, MS**[1,2], **Michael P. Lerario, MD**[1,2], **James K. Min, MD**[3,5], **Costantino Iadecola, MD**[1,2], and **Ajay Gupta, MD**[1,3]

[1]Feil Family Brain and Mind Research Institute, Weill Cornell Medicine

[2]Department of Neurology, Weill Cornell Medicine

[3]Department of Radiology, Weill Cornell Medicine

[4]Department of Healthcare Policy and Research, Weill Cornell Medicine

[5]Dalio Institute of Cardiovascular Imaging, Weill Cornell Medicine

Abstract

Objective—Since some cryptogenic strokes may result from large-artery atherosclerosis that goes unrecognized because it causes <50% luminal stenosis, we compared the prevalence of nonstenosing intracranial atherosclerotic plaques ipsilateral to cryptogenic cerebral infarcts versus the unaffected side using imaging biomarkers of calcium burden.

Methods—In a prospective stroke registry, we identified patients with cerebral infarction limited to the territory of one internal carotid artery (ICA). We included patients with stroke of undetermined etiology and, as controls, patients with cardioembolic stroke. We used noncontrast computed tomography (CT) to measure calcification in both intracranial ICAs including qualitative calcium scoring and quantitative scoring utilizing Agatston-Janowitz (AJ) calcium scoring. Within subjects, the Wilcoxon signed rank sum test for non-parametric paired data was used to compare the calcium burden in the ICA upstream of the infarction versus the ICA on the unaffected side.

Results—We obtained 440 calcium measures from 110 ICAs in 55 patients. Among 34 patients with stroke of undetermined etiology, we found greater calcium in the ICA *ipsilateral* to the infarction (mean Modified Woodcock Visual Score, 6.7 ± 4.6) compared to the *contralateral* side (5.4 ± 4.1) ($P = 0.005$). Among 21 patients with cardioembolic stroke, we found no difference in calcium burden ipsilateral to the infarction (6.7 ± 5.9) versus the contralateral side (7.3 ± 6.3) ($P = 0.13$). Results were similar using quantitative calcium measurements including AJ calcium scores.

Corresponding Author: Hooman Kamel, MD, 407 East 61st St, New York, NY 10065 USA, Phone: 212-746-0382; fax: 212-746-5509, hok9010@med.cornell.edu.

Conflicts of Interests/Disclosures: The authors report no disclosures pertaining to the work under consideration

Conclusion—In patients with strokes of undetermined etiology, the burden of calcified intracranial large-artery plaque was associated with downstream cerebral infarction.

Keywords

Cryptogenic Stroke; Intracranial Atherosclerosis; CT scan; Calcium; Stroke Etiology

One-third of ischemic strokes are classified as cryptogenic because a definite cause cannot be identified.(1) It is increasingly recognized that many cryptogenic strokes arise from a distant thromboembolic source, not in-situ cerebrovascular disease. This has prompted the formulation of an entity called embolic stroke of undetermined source (ESUS), which likely involves a mixture of occult cardiac embolism and artery-to-artery embolism.(2)

The most common cause of artery-to-artery embolism is atherosclerosis. The current criterion for diagnosing atherosclerotic artery-to-artery embolism requires a plaque to have caused ≥50% stenosis of the arterial lumen.(3) However, recent studies suggest that artery-to-artery embolism can occur from vulnerable plaque elements in the extracranial internal carotid artery (ICA) even in the absence of significant luminal narrowing.(4,5) It is unknown whether nonstenosing atherosclerotic lesions in the *intracranial* ICA are also associated with stroke.

More widespread recognition that large-artery atherosclerosis can cause artery-to-artery embolism without causing luminal narrowing would have several implications. It would suggest that updated diagnostic criteria for large-vessel stroke might account for many strokes that are currently classified as cryptogenic. This could extend to a new group of patients the benefits of treatments that appear effective in those with currently recognized large-artery atherosclerosis.(6,7) Therefore, we examined whether nonstenosing atherosclerosis of the intracranial ICA is associated with downstream cerebral infarction.

Methods

Design

If nonstenosing intracranial plaques *cause* some proportion of cryptogenic strokes, these strokes should more often occur downstream of such plaques than downstream of vessels without such plaque. We therefore tested the hypothesis that atherosclerotic plaque is more common upstream of a cryptogenic cerebral infarction than it is upstream of the unaffected hemisphere. In other words, we hypothesized that a patient with a cryptogenic stroke affecting the left cerebral hemisphere would be more likely to harbor a higher burden of atherosclerotic plaque in the *left* intracranial ICA, upstream of the infarct, than in the *right* intracranial ICA. As a further control, we included a cohort of patients with cardioembolic stroke. We hypothesized that there would not be the same left-versus-right asymmetry in large-artery plaque in these patients, since their stroke arose from a central thrombus in the heart. As our marker of vulnerable atherosclerotic plaque, we used measurements of arterial calcification, which has been established as a marker of atherosclerosis, especially in the coronary arteries, and more recently has been shown to be a marker of overall stroke risk.(8)

Our study was approved by the Weill Cornell Medical College institutional review board, which waived the requirement for informed consent.

Subjects

All patients with acute ischemic stroke admitted to the New York-Presbyterian Hospital/ Weill Cornell Medical Center during 2013 were prospectively included in the American Heart Association's (AHA) Get With the Guidelines (GWTG) Stroke registry.(9) Patients were registered after their attending vascular neurologist confirmed the diagnosis of ischemic stroke, defined as an episode of cerebral dysfunction with neuroimaging evidence of infarction or clinical symptoms persisting >24 hours without an obvious nonvascular cause.

Using the Trial of Org 10172 in Acute Stroke Treatment (TOAST) classification scheme,(3) two neurologists used all available medical records to independently assign a stroke etiology. A third neurologist independently resolved any disagreements regarding the classification. Since we were interested in whether cryptogenic strokes can be caused by undiagnosed atherosclerosis, we included all patients with a stroke of undetermined etiology. As a control group, we included patients with cardioembolic strokes because their pathophysiological basis did not involve arterial disease. Because we were interested in *occult* atherosclerotic disease, we excluded strokes whose etiology was recognized as large-artery atherosclerosis based on ≥50% luminal stenosis as required by the TOAST classification. We excluded small-vessel occlusion and strokes due to another determined etiology due to relatively small numbers of cases.

Since we were interested in arterial calcification in the intracranial ICA, from among otherwise eligible patients with stroke of undetermined etiology or cardioembolic stroke, we included only those who underwent noncontrast head computed tomography (CT) with 2.5-mm slice thickness and who had unilateral infarction in one ICA territory.

Clinical Measurements

Trained hospital personnel used standardized methods to prospectively collect data regarding demographics, the NIH Stroke Scale score on admission, and vascular risk factors: tobacco use, diabetes, hypertension, dyslipidemia, atrial fibrillation, congestive heart failure, coronary heart disease, peripheral vascular disease, and cardiac valvular disease.

CT Imaging Technique

All head CT studies were performed on one of the General Electric CT scanners at our institution: the Optima 660, Light Speed Xtra, Discovery HD 750, or the Light Speed Pro. Imaging was performed according to the standard protocol used during this time period for patients referred for a suspected or known acute stroke. The head CT coverage extended from the foramen magnum to the skull vertex with a display field-of-view of 22 cm. Scans were performed using 120 kVp and mA ranging from 250 to 300. All images were reconstructed at 2.5 mm axial sections. In cases with multiple CT studies, we used the CT performed closest to the time of admission for stroke.

Calcium Scoring Protocol—For both qualitative and semi-automated quantitative calcium scoring, we assessed the severity of arterial calcification separately for each ICA beginning inferiorly just above its exit from the petrous temporal bone and ending superiorly at the level of the terminal ICA bifurcation. The petrous segment of the ICA within the temporal bone was excluded because of difficulty in separating arterial calcification from adjacent bone in this segment. The middle cerebral arteries were excluded because calcification rarely occurs in this location in the absence of significant luminal stenosis. A single neuroradiologist interpreted research imaging studies without knowledge of clinical or other imaging data. The exclusive use of bone windows allowed calcium scoring to occur without knowledge of infarct location.

Qualitative Visual Calcium Scoring—We used a recently validated qualitative calcium scoring method, the Modified Woodcock Visual Scoring (MWVS) scale.(10,11) The MWVS scale assigns a score reflecting the severity of calcification on each axial slice in which the ICA is visible, starting just distal to the petrous temporal bone and ending at the level of the terminal bifurcation. A score of 0 reflects no calcification; 1 reflects thin, discontinuous calcification; 2 reflects thin and continuous or thick and discontinuous calcification; and 3 reflects thick, continuous calcification (Figure 1). Scores for each axial slice were summed to create separate MWVS scores for the right and left ICA in each subject. To assess reproducibility, a second radiologist independently reassessed a subset of 50 MWVS scores in our cohort.

Semi-Automated Quantitative Calcium Scoring—Imaging data were transferred to a General Electric AW2 server and analyzed using Smartscore 4.0 software (GE Healthcare, USA), a commercially available program for evaluating coronary calcium scores. We used the Smartscore software to calculate the Agatston-Janowitz (AJ) 130 calcium score,(12) the calcium volume, and the estimated mass of arterial calcification associated with each patient's left and right ICA. On each axial slice of the ICA from the level just above the petrous apex up to the terminal bifurcation, a neuroradiologist used a manual drawing tool in the Smartscore 4.0 software suite to circle the region containing visible calcifications, taking care to exclude adjacent bone from the region of interest (Figure 1). The software identified calcifications as any region with a Hounsfield unit (HU) value >130. The area of these calcifications was multiplied by a density factor (130–199 HU: 1; 200–299 HU: 2; 300–399 HU: 3; 400+ HU: 4) to provide a calcium score for each slice. Scores were summed over all slices with visible calcium for each ICA. The software also provided a calculated volume of calcium by multiplying the number of voxels with HU values >130 and summing the total voxel volumes for each ICA. Based on both volume and density calculations, the software automatically generated an estimated mass of the calcium above 130 HU. A second radiologist independently drew ROIs to reassess reproducibility in a subset of 25 AJ-130 measurements.

Statistical Analysis

By comparing the calcium burden upstream of an infarct versus in the ICA on the unaffected side, we were able to isolate the effect of ICA atherosclerosis on stroke risk while reducing the risk of unmeasured confounding that can occur in between-patient comparisons, since

each patient's contralateral artery served as a control for the artery upstream of the infarction. For this design, we used the Wilcoxon signed rank sum test for non-parametric paired data. We used this technique to assess MWVS score, AJ-130 score, calcium volume, and calcium mass. These analyses were first performed in patients with cryptogenic stroke, and then separately in patients with cardioembolic stroke. We then used the Wilcoxon-Mann-Whitney test to evaluate the hypothesis that patients with stroke of undetermined etiology (as compared to those with cardioembolic stroke) had a larger asymmetry in calcium burden between the ICA upstream of their infarct compared to the unaffected ICA.

For descriptive analyses of the baseline characteristics of patients with cryptogenic stroke versus cardioembolic stroke, we used the chi-square or Fisher's exact test for categorical variables and the t-test or Wilcoxon-Mann-Whitney test for continuous variables. To assess interobserver reliability, we assessed a Kappa coefficient for the MWVS scale and an intraclass correlation coefficient for the AJ-130 score. Linear regression was used to assess the relationship between MWVS score and AJ-130 score. All *P* values are two-sided and were evaluated at $\alpha = 0.05$. All analyses were performed using SAS v9.3 (SAS Institute, Cary, NC).

Results

Baseline Patient Characteristics and Diagnostic Evaluations

Our institution's GWTG Stroke registry included 346 patients with ischemic stroke in 2013, of whom 92 (34.4%) had a stroke of undetermined cause and 105 (39.3%) had a cardioembolic stroke. Of these 197 patients, we included the 55 who had a head CT with 2.5-mm slice thickness and unilateral infarction in the anterior circulation. As expected, those with cardioembolic stroke had a significantly higher prevalence of atrial fibrillation than patients with cryptogenic stroke, but these two groups were otherwise comparable in regards to demographics, other vascular risk factors, and the extent of diagnostic evaluation (Table 1). The median interval between the day of admission and performance of the head CT for calcium scoring was 1 day.

Imaging Results

The correlation coefficient between the MWVS score and the AJ-130 calcium score was 0.89, indicating a strong linear relationship between our two main approaches for assessing calcium burden (Figure 2). Measures of reproducibility demonstrated a kappa coefficient of 0.89 (95% CI 0.78–0.99) for the MWVS score and an intraclass correlation coefficient of 0.99 for the AJ-130 score (95% CI 0.995–0.999), indicating outstanding inter-observer reproducibility.

In patients with a stroke of undetermined etiology, we found a substantially greater qualitative calcium burden in the ICA *upstream* of the infarct (mean MWVS score, 6.7 ± 4.6) as compared to the ICA on the *unaffected* side (mean MWVS score, 5.4 ± 4.1; $P = 0.005$). In these patients, we found the same pattern in regards to quantitative measurements of calcium burden (Table 2). Conversely, in the control group of patients with cardioembolic stroke, we found no difference in the calcium burden upstream of the infarction (mean

MWVS score, 6.7 ± 5.9) as compared to the unaffected side (mean MWVS score, 7.3 ± 6.3; $P = 0.13$). In these patients, there were also no significant differences in any of the quantitative measures of calcium burden between the upstream ICA versus the unaffected vascular territory (Table 2).

Discussion

In a prospective stroke registry, we found an association between upstream large-artery atherosclerosis and downstream cerebral infarctions that were classified as cryptogenic according to current diagnostic criteria. Conversely, we found no such association between upstream atherosclerosis and downstream infarction among patients with cardioembolic stroke. Our findings suggest that some proportion of strokes from large-artery intracranial atherosclerosis are currently not being recognized as such because the atherosclerotic plaque has not caused 50% stenosis of the arterial lumen.

Our findings should be interpreted in light of recent studies on potential causes of cryptogenic stroke. Based on clinical and radiographic features, it is thought that many cryptogenic strokes reflect occult thromboembolism from arterial sources other than aortic arch atheroma, which has long been associated with stroke.(2) Although case reports and case series have raised the hypothesis that nonstenosing plaque of the cervical and intracranial arteries may cause downstream artery-to-artery embolism, these analyses lacked the control groups needed to support a causal relationship.(13–17) We and others found a higher burden of vulnerable atherosclerotic plaque in the cervical ICA upstream of cryptogenic cerebral infarctions as compared to the unaffected ICA,(4,5) which more directly supports the hypothesis that some cryptogenic strokes may arise from unrecognized nonstenosing plaques. On the other hand, a recent analysis from a large population-based study argued against occult atherosclerotic disease as a cause of cryptogenic stroke.(18) This study lacked detailed imaging of high-risk plaque elements and instead used ultrasonographic assessments of luminal stenosis and indirect assessments such as lipid profiles. Another recent study found that patients with nonlacunar stroke did not manifest a greater calcium burden upstream of their infarction than patients with lacunar stroke.(19) This between-patients comparison may be subject to residual confounding because the lacunar stroke patients may have had a substantial burden of co-existing atherosclerotic disease. In this context, our findings lend weight to the hypothesis that culprit large-artery lesions do exist which could explain many cryptogenic strokes, but that we need to use better markers of high-risk plaque than simply relying on the degree of luminal stenosis.

The criterion of luminal stenosis appears to stem from risk-benefit calculations regarding carotid endarterectomy(6) rather than pathophysiological considerations, and yet it remains a mainstay of stroke classification schemes.(3,20,21) Our findings support research to identify better markers of culprit atherosclerotic plaque, such as magnetic resonance imaging of the vessel wall. In the meantime, our findings support the use of stroke classification schemes such as the Causative Classification System (CCS), which takes into account plaque morphology in addition to the degree of luminal stenosis.(21) Our results support a more rigorous analysis of atherosclerotic calcification on noncontrast head CT exams, since these studies are almost universally obtained in the diagnostic evaluation of patients with known

or suspected acute ischemic stroke. Noncontrast head CT also provides the benefit of quantitative markers of calcium burden, including the semi-automated AJ-130 measures of calcium score, volume, and mass. The usefulness of each of these specific quantitative measures as a tool for providing insight into plaque biology requires further investigation. For example, unlike mass or density measures, ICA calcium volumes might show an association with the positive vessel remodeling and ectasia known to occur in intracranial atherosclerotic disease.

Improving the detection of atherosclerotic plaque as the underlying cause of stroke is not simply an academic matter, but rather an issue with immediate clinical implications. For example, guidelines from the American Heart Association recommend intensive statin therapy for secondary stroke prevention only if a stroke or transient ischemic attack is presumed to be of atherosclerotic origin.(22) Failure to appreciate an underlying atherosclerotic plaque may therefore preclude any number of promising therapies for preventing recurrent stroke.(6,7) Future prospective studies are now warranted to further identify promising markers of high-risk nonstenosing plaque, elucidate the mechanisms of stroke in such patients, and prove that patients harboring culprit nonstenosing plaques have a risk of stroke recurrence high enough to warrant the initiation of more aggressive stroke prevention therapies.

Our study has several limitations. First, our stroke subtype classifications were retrospective. We minimized classification bias by using three independent adjudicators blinded to the study hypothesis. Second, the noncontrast head CTs we used to assess calcium burden can also provide evidence on the location of infarction, thereby potentially introducing the risk of assessment bias in our analysis. However, we exclusively used CT bone windows in our calcium score assessments, which minimized the risk of such bias since the relatively subtle CT imaging findings present in an acute ischemic infarction are very difficult to detect on bone windows. Furthermore, assessment bias is unlikely to explain our results because assessment of neuroimaging occurred completely blinded to stroke etiology. Third, this was a retrospective single-center study with a relatively small sample of mostly white patients, and future work will be needed to build on these findings in larger, more heterogeneous, prospective cohorts. Fourth, we used the TOAST classification system instead of the CCS classification system, which allows more liberal inclusion of nonstenosing atherosclerotic plaques.(3,21) However, the TOAST criteria and the ASCO criteria(20) remain in common use, attesting to the enduring power of the ≥50% stenosis criterion. By using the TOAST criteria, we were able to show that common conceptions of stroke etiology may lead to misclassification of strokes as cryptogenic when in fact they are due to large-artery atherosclerosis.

Conclusions

We found an association between the burden of calcified intracranial large-artery plaque and downstream cerebral infarction in patients with strokes of undetermined etiology. These findings support the hypothesis that undiagnosed, nonstenosing atherosclerotic lesions may explain some proportion of cryptogenic strokes and that the detection of these atherosclerotic disease is possible using noncontrast head CT.

Acknowledgments

Sources of Funding: Supported by grants K23NS082367 (Kamel), K23NS091395 (Navi), R01NS034179 (Iadecola), and KL2TR000458 (Gupta) from the National Institutes of Health.

None.

References

1. Marnane M, Duggan CA, Sheehan OC, et al. Stroke subtype classification to mechanism-specific and undetermined categories by TOAST, A-S-C-O, and Causative Classification system. Stroke. 2010; 41:1579–1586. [PubMed: 20595675]
2. Hart RG, Diener HC, Coutts SB, et al. Embolic strokes of undetermined source: the case for a new clinical construct. Lancet Neurol. 2014; 13:429–38. [PubMed: 24646875]
3. Adams HP Jr, Bendixen BH, Kappelle LJ, et al. Classification of subtype of acute ischemic stroke. Definitions for use in a multicenter clinical trial. TOAST. Trial of Org 10172 in Acute Stroke Treatment. Stroke. 1993; 24:35–41. [PubMed: 7678184]
4. Freilinger TM, Schindler A, Schmidt C, et al. Prevalence of nonstenosing, complicated atherosclerotic plaques in cryptogenic stroke. JACC Cardiovascular imaging. 2012; 5:397–405. [PubMed: 22498329]
5. Gupta A, Gialdini G, Lerario MP, et al. Magnetic resonance angiography detection of abnormal carotid artery plaque in patients with cryptogenic stroke. Journal of the American Heart Association. 2015; 4:e002012. [PubMed: 26077590]
6. Chimowitz MI, Lynn MJ, Derdeyn CP, et al. Stenting versus aggressive medical therapy for intracranial arterial stenosis. N Engl J Med. 2011; 365:993–1003. [PubMed: 21899409]
7. Amarenco P, Bogousslavsky J, Callahan A 3rd, et al. High-dose atorvastatin after stroke or transient ischemic attack. N Engl J Med. 2006; 355:549–59. [PubMed: 16899775]
8. Bos D, Portegies ML, van der Lugt A, et al. Intracranial carotid artery atherosclerosis and the risk of stroke in whites: the Rotterdam Study. JAMA Neurol. 2014; 71:405–11. [PubMed: 24535643]
9. Saver JL, Fonarow GC, Smith EE, et al. Time to treatment with intravenous tissue plasminogen activator and outcome from acute ischemic stroke. JAMA. 2013; 309:2480–8. [PubMed: 23780461]
10. Subedi D, Zishan US, Chappell F, et al. Intracranial Carotid Calcification on Cranial Computed Tomography: Visual Scoring Methods, Semiautomated Scores, and Volume Measurements in Patients With Stroke. Stroke. 2015; 46:2504–9. [PubMed: 26251250]
11. Woodcock RJ Jr, Goldstein JH, Kallmes DF, Cloft HJ, Phillips CD. Angiographic correlation of CT calcification in the carotid siphon. AJNR Am J Neuroradiol. 1999; 20:495–9. [PubMed: 10219418]
12. Agatston AS, Janowitz WR, Hildner FJ, Zusmer NR, Viamonte M Jr, Detrano R. Quantification of coronary artery calcium using ultrafast computed tomography. J Am Coll Cardiol. 1990; 15:827–32. [PubMed: 2407762]
13. Schwarz F, Bayer-Karpinska A, Poppert H, et al. Serial carotid MRI identifies rupture of a vulnerable plaque resulting in amaurosis fugax. Neurology. 2013; 80:1171–2. [PubMed: 23509049]
14. Trivedi RA, JMUK-I, Graves MJ, Gillard J, Kirkpatrick PJ. Non-stenotic ruptured atherosclerotic plaque causing thrombo-embolic stroke. Cerebrovasc Dis. 2005; 20:53–5.
15. Olsen TS, Skriver EB, Herning M. Cause of cerebral infarction in the carotid territory. Its relation to the size and the location of the infarct and to the underlying vascular lesion. Stroke. 1985; 16:459–66. [PubMed: 4002261]
16. Nakamura T, Tsutsumi Y, Shimizu Y, Uchiyama S. Ulcerated carotid plaques with ultrasonic echolucency are causatively associated with thromboembolic cerebrovascular events. J Stroke Cerebrovasc Dis. 2013; 22:93–9. [PubMed: 21820918]
17. Kim JS, Nah HW, Park SM, et al. Risk factors and stroke mechanisms in atherosclerotic stroke: intracranial compared with extracranial and anterior compared with posterior circulation disease. Stroke. 2012; 43:3313–8. [PubMed: 23160885]

18. Li L, Yiin GS, Geraghty OC, et al. Incidence, outcome, risk factors, and long-term prognosis of cryptogenic transient ischaemic attack and ischaemic stroke: a population-based study. Lancet Neurol. 2015; 14:903–13. [PubMed: 26227434]

19. van Dijk AC, Fonville S, Zadi T, et al. Association between arterial calcifications and nonlacunar and lacunar ischemic strokes. Stroke. 2014; 45:728–33. [PubMed: 24457294]

20. Amarenco P, Bogousslavsky J, Caplan LR, Donnan GA, Wolf ME, Hennerici MG. The ASCOD phenotyping of ischemic stroke (Updated ASCO Phenotyping). Cerebrovasc Dis. 2013; 36:1–5.

21. Ay H, Benner T, Arsava EM, et al. A computerized algorithm for etiologic classification of ischemic stroke: the Causative Classification of Stroke System. Stroke. 2007; 38:2979–84. [PubMed: 17901381]

22. Kernan WN, Ovbiagele B, Black HR, et al. Guidelines for the prevention of stroke in patients with stroke and transient ischemic attack: a guideline for healthcare professionals from the American Heart Association/American Stroke Association. Stroke. 2014; 45:2160–236. [PubMed: 24788967]

COMPETENCY IN MEDICAL KNOWLEDGE

Using a simple noncontrast head CT imaging technique, this study demonstrated a strong association between non-stenosing intracranial ICA calcification and ipsilateral acute brain infarction. Non-stenosing carotid atherosclerotic lesions measured by both qualitative assessment and existing calcium scoring techniques may be useful diagnostic techniques to explain the etiology of some proportion of cryptogenic strokes.

TRANSLATIONAL OUTLOOK

Further studies are warranted to determine whether patients currently labeled as having a cryptogenic stroke but who harbor a potential causative non-stenosing carotid atherosclerosis may benefit from intensified and targeted therapy aimed at reducing their vascular risk.

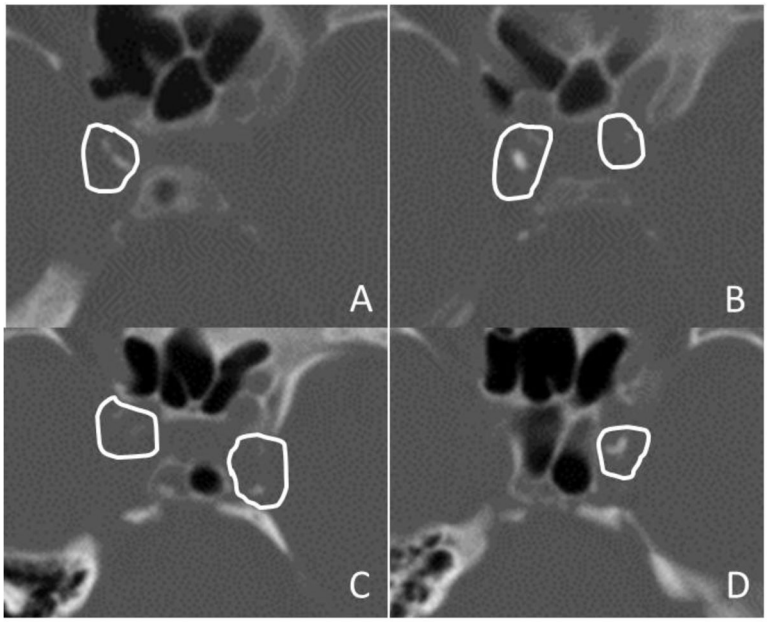

Figure 1. Representative Computed Tomography Images

Images are shown in bone windows from two patients with intracranial internal carotid artery (ICA) calcifications.

Panels A and B. Two contiguous axial images from Patient 1 in panels A and B show manually drawn regions of interest surrounding ICA calcification, with care taken to avoid including adjacent skull structures. This patient had Modified Woodcock Visual Scale (MWVS) scores of 2 and 3 for the right ICA (A) and 0 and 1 for the left ICA (B). The total Agatston-Janowitz (AJ) 130 score was 334 for the right ICA and 23 for the left. This patient had a right-sided acute anterior circulation infarction.

Panels C and D. Two contiguous axial images from Patient 2 in panels C and D show similarly drawn regions of interest surrounding ICA calcifications. This patient had MWVS scores of 1 and 0 for the right ICA (C) and 2 and 3 for the left ICA (D). The total AJ-130 score was 84 for the right ICA and 198 for the left. This patient had a left-sided acute anterior circulation infarction.

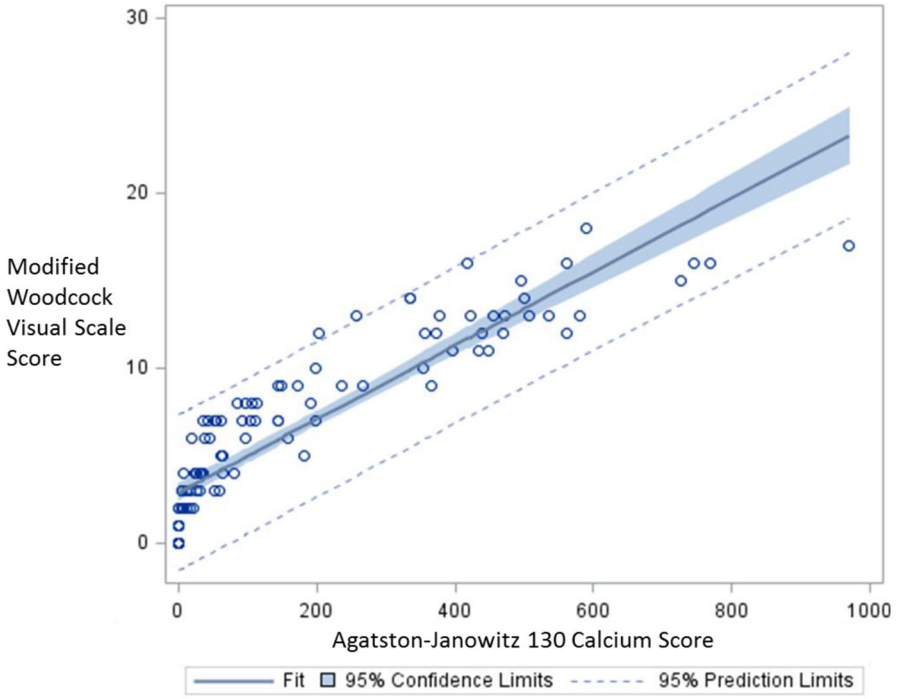

Figure 2.

Scatterplot of Correlation between Agatston-Janowitz 130 Calcium Scores and Modified Woodcock Visual Scale Scores.

Table 1

Baseline Characteristics of Patients, Stratified by Stroke Subtype

Characteristic*	Overall (N=55)	Cardioembolic (N=21)	Undetermined Etiology (N=34)	P value†
Age, mean (SD), years	71.9(15.1)	71.3(15.8)	72.4(14.8)	0.80
Female	36 (65.5)	16(76.2)	20 (58.8)	0.19
Race:				0.66
White	49(89.1)	20 (95.2)	29 (85.3)	
Black	4 (7.3)	1 (4.8)	3 (8.8)	
Other	2 (3.6)	0(0)	2 (5.9)	
Insurance:				0.77
Commercial	13 (23.6)	5 (23.8)	8 (23.5)	
Medicare	26 (47.3)	11 (52.4)	15(44.1)	
Medicaid	16(29.1)	5 (23.8)	11 (32.4)	
Atrial fibrillation	19 (34.6)	16(76.2)	3 (8.8)≠	<0.001
Congestive heart failure	7(12.7)	7 (33.3)	0 (0.0)	0.001
Coronary heart disease	11 (20.0)	5 (23.8)	6(17.7)	0.58
Valvular disease	1 (1.8)	1 (4.8)	0(0)	0.38
Peripheral vascular disease	2 (3.6)	2 (9.5)	0(0)	0.14
Diabetes	15(27.3)	5 (23.8)	10 (29.4)	0.65
Hypertension	39 (70.9)	13(61.9)	26 (76.5)	0.25
Dyslipidemia	31 (56.4)	10(47.6)	21 (61.8)	0.30
Prior stroke	12(21.8)	5 (23.8)	7 (20.6)	0.99
Active tobacco use	3 (5.5)	1 (4.8)	2 (5.9)	0.99
Intravenous thrombolysis	8(14.6)	4(19.1)	4(11.8)	0.46
NIHSS score, median (IQR)	4(3–12)	6(5–14)	4(2–7)	0.09
12-lead electrocardiogram	55(100.0)	21 (100.0)	34(100.0)	0.99
Heart-rhythm monitoring for ≥24 hrs	55(100.0)	21 (100.0)	34(100.0)	0.99
Echocardiogram	48 (87.3)	15(71.4)	33(97.1)	0.01
Echocardiogram type:				0.62
Transthoracic	42 (87.5)	13 (86.7)	29 (87.9)	
Transesophageal	2 (4.2)	0(0)	2(6.1)	
Both	4 (8.3)	2(13.3)	2(6.1)	
Extracranial vascular imaging	55(100.0)	21 (100.0)	34(100.0)	0.99
Intracranial vascular imaging	55(100.0)	21 (100.0)	34(100.0)	0.99
Time to head CT, mean (SD), days	0.9(1.1)	1.4 (1.3)	0.6 (0.7)	0.01

Abbreviations: CT, computed tomography; IQR, interquartile range; NIHSS, NIH Stroke Scale; SD, standard deviation.

*All data are presented as numbers (%) unless otherwise indicated.

†*P* value by chi-square/Fisher's exact or t-test/Wilcoxon-Mann-Whitney, where appropriate.

[≠]Despite the presence of atrial fibrillation, these three cases were adjudicated as being of undetermined etiology due to multiple potential causes of stroke.

Table 2

Measures of Calcium Burden Upstream of Cerebral Infarction Compared to the Unaffected Side

Measure	Upstream of Infarction	Unaffected Side	Difference	*P* value*
Strokes of undetermined etiology:				
MWVS score:				
Mean (SD)	6.7 (4.6)	5.4(4.1)	1.3(2.6)	0.005
Median (IQR)	7(3–9)	4.5 (2–7)		
AJ-130 score:				
Mean (SD)	158.3(192.6)	124.2(198.1)	34.1 (87.7)	0.006
Median (IQR)	71.5(22–235)	36.5(7–144)		
Calcium mass:				
Mean (SD)	25.0(28.1)	21.4(32.7)	3.6(16.5)	0.04
Median (IQR)	16(3–41)	7.5(1–21)		
Calcium volume:				
Mean (SD)	55.9(28.1)	46.7(61.6)	9.3 (30.2)	0.02
Median (IQR)	34(11–98)	23(6–51)		
Cardioembolic strokes:				
MWVS score:				
Mean (SD)	6.7 (5.9)	7.3 (6.3)	−0.6(2.1)	0.13
Median (IQR)	7(0–13)	6(1–14)		
AJ-130 score:				
Mean (SD)	211.5(254.2)	213.4(241.1)	−2.0 (−126.6)	0.63
Median (IQR)	98 (0–377)	64 (0–447)		
Calcium mass:				
Mean (SD)	33.3(41.2)	35.1 (40.2)	−1.8(23.0)	0.34
Median (IQR)	4(0–51)	19(0–53)		
Calcium volume:				
Mean (SD)	68.2 (78.6)	70.5 (74.9)	−2.2(31.7)	0.53
Median (IQR)	47(0–118)	45(0–123)		

Abbreviations: AJ, Agatston-Janowitz; IQR, interquartile range; MWVS, Modified Woodcock Visual Scale; SD, standard deviation.

* *P* value by Wilcoxon signed rank sum test for non-parametric paired data.